Microsc. Microanal., page 1 of 8
doi:10.1017/S1431927616000659

Microscopy AND Microanalysis

Picoliter Drop-On-Demand Dispensing for Multiplex Liquid Cell Transmission Electron Microscopy

Joseph P. Patterson,[1,a] Lucas R. Parent,[1,a] Joshua Cantlon,[2] Holger Eickhoff,[2] Guido Bared,[2] James E. Evans,[3] and Nathan C. Gianneschi[1,*]

[1]*Department of Chemistry & Biochemistry, University of California San Diego, La Jolla, CA 92093, USA*
[2]*SCIENION AG, Volmerstr. 7a, 12489 Berlin, Germany*
[3]*Environmental Molecular Science Laboratory, Pacific Northwest National Laboratory, 3335 Innovation Blvd., Richland, WA 99354, USA*

Abstract: Liquid cell transmission electron microscopy (LCTEM) provides a unique insight into the dynamics of nanomaterials in solution. Controlling the addition of multiple solutions to the liquid cell remains a key hurdle in our ability to increase throughput and to study processes dependent on solution mixing including chemical reactions. Here, we report that a piezo dispensing technique allows for mixing of multiple solutions directly within the viewing area. This technique permits deposition of 50 pL droplets of various aqueous solutions onto the liquid cell window, before assembly of the cell in a fully controlled manner. This proof-of-concept study highlights the great potential of picoliter dispensing in combination with LCTEM for observing nanoparticle mixing in the solution phase and the creation of chemical gradients.

Key words: liquid cell transmission electron microscopy, TEM sample preparation, dispensing organic non-organic solutions, grid loading

Introduction

Liquid cell transmission electron microscopy (LCTEM) is bringing about a paradigm shift in the analysis of nanomaterials in solution. For the first time, we can use electron microscopy to not only characterize critical features including particle size and morphology, but to observe liquid-phase dynamics, in real-time with nanometer resolution (Williamson et al., 2003; de & Ross, 2011). LCTEM has shown great potential for advancing our understanding of nanoparticle growth (Zheng et al., 2009*b*; Evans et al., 2011; Woehl et al., 2012; Liao & Zheng, 2013; Liao et al., 2014; Woehl et al., 2014; Patterson et al., 2015*a*; Smeets et al., 2015), and particle–particle interactions (Chen et al., 2015*a*). There has been a particular focus on inorganic nanocrystalline materials such as Au, Pt, and Pd because they provide high contrast and the ability to undergo electron beam-induced growth via radiolysis and metal complex reduction of precursor solutions during the imaging experiments (Evans et al., 2011; Liao & Zheng, 2013; Liao et al., 2014; Woehl et al., 2014). However, increasingly other materials, including ones containing organic components (Proetto et al., 2014) and having low contrast, are being studied. In a typical LCTEM experiment, a liquid sample is deposited onto the surface of a flat silicon nitride chip (ca. $2.5 \times 2.5\ mm^2$) and subsequently sealed off to prevent exposure to the internal vacuum of the electron microscope. The seal is made by placing a second chip on top of the solution and enclosing the chips within a LCTEM holder (de & Ross, 2011). Therefore, the liquid thickness of the cell is set by the size of nanoparticles within the sample, which physically hold the chips apart. If a thicker cell is required, so-called "spacer-chips," which have raised columns on the silicon nitride surface, can be used to physically separate the two silicon nitride surfaces. These spacer-chips allow for the cells to be assembled "in air" (no liquid initially between the chips), and to then flow external liquid into the window region of the cell after insertion in the microscope. Although many reports discuss the great potential of LCTEM for the study of nanoparticle systems formed through the mixing of solutions containing various required components or conditions (de & Ross, 2011; Chen et al., 2015*b*), there has been no demonstration whereby two solutions have been mixed within the viewing windows of the liquid cell, largely due to technical limitations in dispensing and circulating separate liquids within the confined nanoliter volumes typical of the cells. Furthermore, although several holder designs allow the flow of multiple liquids into the tip region of the LCTEM holder using inlet/outlet lines, mixing of the liquids by this method occurs in the collection wells before the mixture reaching the window region of the cell (Nielsen et al., 2014). This inability to control the location and extent of liquid mixing significantly limits our ability to study how chemistry manifests itself on the nanoscale using LCTEM. For example, nanoparticles formed through block copolymer assembly are typically synthesized through a solvent mixing process (Choucair & Eisenberg, 2003; Mai & Eisenberg, 2012; Proetto et al., 2014; Barnhill et al., 2015), whereby particle assembly occurs within seconds of reaching a certain mixing ratio, which is followed by a period of particle relaxation (Barnhill et al., 2015). Unless solution mixing is initiated

Received September 13, 2015; accepted March 7, 2016
*Corresponding author. ngianneschi@ucsd.edu
[a]Contributed equally to this paper.

directly in the window region and in the transmission electron microscopy (TEM) field of view, initial particle assembly cannot be observed. Furthermore, we recently studied the formation of a ZIF-8 metal-organic-framework (MOF) system, which again occurs through solution mixing (Patterson et al., 2015*a*). Due to our inability to mix the components directly in the viewing region of the cell, we miss the initial stages of particle formation, which can occur within the first 15 s(Cravillon et al., 2011).

In this paper, we demonstrate that picoliter drop-on-demand dispensing can be used to controllably load multiple samples onto a single liquid cell window or a cell with an array of windows, which provides the potential to pattern samples for both high-throughput liquid cell experiments, as well as to perform mixing of multiple different solutions inside the cell. We demonstrated this concept by dispensing and imaging solutions of two types of crystalline particles amenable to selected area diffraction for verification of structure during LCTEM. The two particles were also chosen to be morphologically distinguishable by TEM imaging. Therefore, we employed gold nanoparticles (AuNPs) and nanocrystals of the MOF UiO-66 (Patterson et al., 2015*a*). These two particle types were dispensed onto a single liquid cell window where initial mixing occurs upon assembly of the cell and continues through diffusion of the components during *in situ* LCTEM imaging. We propose that the LCTEM technique presented here will open the door for *in situ* nanomaterial synthesis studies that require the mixing of precursor solutions directly in the viewing area, and for studies of responsive nanomaterials that undergo dynamic transformation upon changes in solution conditions and/or constituents.

Materials and Methods

TEM was performed on a FEI Sphera microscope (FEI, Hillsboro, OR, USA) operated at 200 keV. Micrographs were recorded on a 2×2 K Gatan charged-coupled device (CCD) (Gatan Inc., Pleasanton, CA, USA). Movies were recorded at dose rates between 15.0 e nm^2/s (6.7×10^5 Gy/s) and 0.2 e nm^2/s (1.2×10^5 Gy/s). UiO-66 was synthesized and characterized as previously reported (Patterson et al., 2015*a*), and dispersed in water at 5 mg/mL. A quantity of 20 nm AuNPs were purchased from BB International (www.british-biocell.co.uk), EM.GC20, and used as received. LCTEM experiments were carried out with a Hummingbird Scientific Liquid Flow TEM Holder (Hummingbird Scientific, Lacey, WA, USA). Drop-on-demand dispensing was performed on a SciTEM (SCIENION AG, Berlin, Germany). The SciTEM is a liquid-handling platform designed for dispensing volumes as low as 35 pL with a lateral precision of $\pm 2\,\mu$m. These capabilities enable the user to spot up to 10×10 individual spots on a single TEM grid (dimension 1 mm^2). The spot positions can be easily positioned using a multipoint touch screen and optical camera system specifically designed to recognize TEM grids. All steps are captured and recorded by three independent cameras: the DropCam controls drop formation, stability, and volume; the GlobalCam enables intuitive selection of the target grids; and the high-resolution HeadCam allows precise fiducial-aided drop positioning. Unlike other picoliter printing systems, the SciTEM's unique nozzle design, which is made of medical-grade borosilicate glass, exhibits a round orifice with no edges. This eliminates the onset of crystallization, minimizing the chance for drop deviation. The nozzles have an orifice ranging between 50 and 80 μm, depending on the nozzle type. This allows the SciTEM to dispense both nanomaterials and microstructures up to 20 μm in diameter without clogging (i.e., carbon nanotubes, catalysts, and quantum dots). In contrast to other dispense technologies, SCIENION's dispensers do not impose a strong shock wave on the sample and thus create minimal shear forces: for example, living eukaryotic cells can be dispensed without altering their viability. All liquid-handling parts are composed of inert materials: PEEK®, Teflon®, and glass. The liquid phase can be freely changed from aqueous to organic solvents to allow printing of aqueous and organic samples, respectively. Four coatings have been developed to modify the nozzle's surface energy to enable stable drop formation of various sample types without the need to change the sample properties. The SciTEM can dispense solutions within a viscosity range of 0.4–6 mPa.s.

Results and Discussion

Dispensing of low-volume liquids has been used for many scientific applications including high-throughput mass spectrometry analysis (Aerni et al., 2006), low-volume synthesis (Wixforth et al., 2004), the preparation of materials through inkjet printing of polymer/inorganic materials (Calvert, 2001; de Gans et al., 2004; Tekin et al., 2008), and biosensing applications (Li et al., 2015). The development of these approaches is of interest to the field of LCTEM for their ability to fully automate the dispensing of nano- or picoliter volumes of liquid in a controlled manner. The SciTEM used in this work is an automated picoliter drop-on-demand dispensing instrument capable of recognizing and aligning TEM grids to be decorated with multiple and varied samples by dispensing liquid droplets down to 35 pL and allowing them to dry directly on the grid. Depending on the surface hydrophobicity of the substrate, droplets will either spread over large areas or remain as high-contact angle ellipsoids. Typically, an array of such low-volume droplets on a hydrophobic surface (e.g., silicon nitride) will evaporate within a few seconds (and even faster for hydrophilic surfaces), much too quickly to allow sealing of the liquid cell after deposition without complete or significant dehydration of the samples. However, if an array of water droplets is first dispensed around the sample area, the evaporation of these water droplets creates a local high-humidity microenvironment, greatly reducing evaporation rates of the sample droplets (Fig. 1, Supplementary Movie 1). This method of controlled water array dispensing to create stable droplets of sample solution, which persist for ~1 min, provides

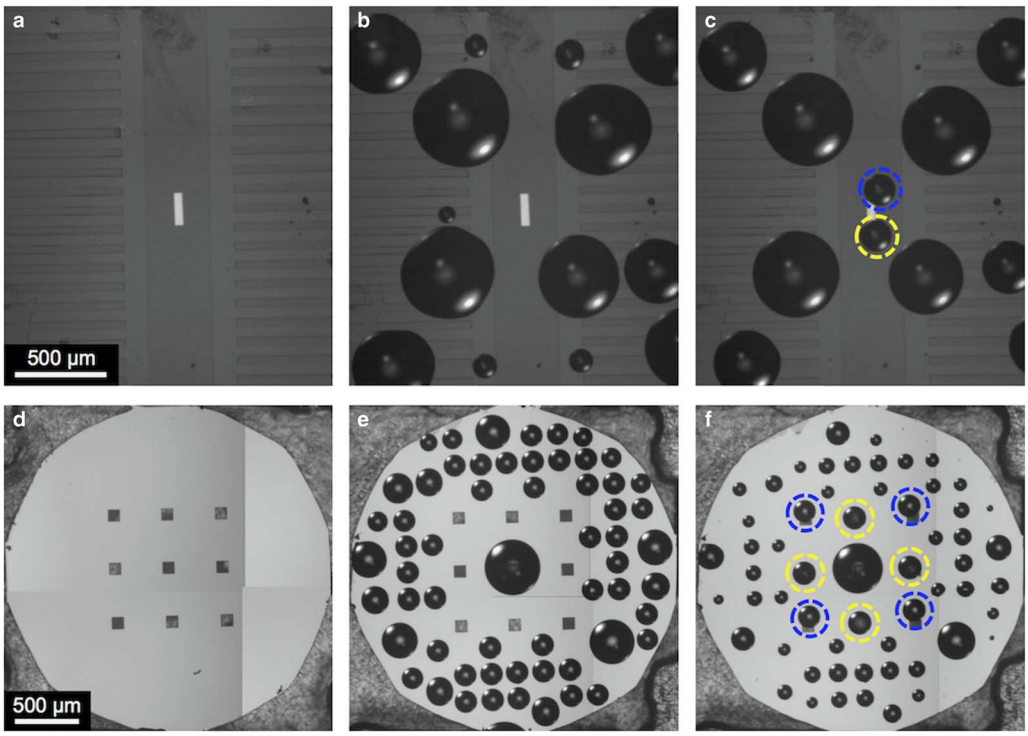

Figure 1. Optical images of Hummingbird Scientific 200 nm spacer-chips with a single 50 nm thick, $200 \times 50\,\mu$m window (**a–c**) and a Norcada 10 nm thick $100 \times 100\,\mu$m, nine window array (**d–f**), showing the windows predeposition (**a,d**), postdeposition of pure water to create a high-humidity environment (**b,e**) and postdeposition of 20 nm gold nanoparticles (yellow) and 200 nm UiO-66 (blue) (**c,f**).

sufficient time to seal the liquid cell and ensure that the samples remain hydrated. We note, however, that this could also be achieved by dispensing onto substrates inside a controlled humidity chamber, and work is underway to develop this additional capability into the SciTEM.

Supplementary Movie 1

Supplementary Movie 1 can be found online. Please visit journals.cambridge.org/jid_MAM.

Various array designs can be imagined, utilizing different TEM grids, in order to dispense multiple picoliter sample volumes onto a single channel for controlled mixing (Figs. 1a–1c) or, to dispense multiple separate samples onto a single grid for high-throughput analysis (Figs. 1d–1f). In a proof-of-concept demonstration, we used this method to observe progressive diffusion mixing of a 20 nm AuNP solution and a MOF UiO-66 solution (both in H_2O). For the initial test, after dispensing the array (Fig. 1c), the solution droplets were left to dry (Supplementary Movie 1) and the window was imaged under vacuum to show full separation of the AuNPs and MOF nanoparticles (Fig. 2), that match very well the optical images of the dispensed droplets (Fig. 1c). Particle type was confirmed both by imaging the morphology and size of the particles and via selected area diffraction (Fig. 2). This demonstrates that even with conventional, commercially available liquid cell chips, two different liquid samples can both be dispensed over the imaging window ($200 \times 50\,\mu$m) while still being isolated from each other before sealing the holder, at which point mixing would be initiated due to the lateral spreading of each droplet.

To create a hydrated liquid cell for *in situ* TEM observation, we dispensed picoliter droplets of the two samples onto a single chip using the same two sample array and $200 \times 50\,\mu$m imaging window (Fig. 1c), intending to quickly seal the cell before sample evaporation. The sample and water droplets were all dispensed within a 2-min time period, and the cell was sealed in the liquid stage tip ~20 s after the two sample droplets were dispensed. At the moment of sealing the sample droplets under the top chip, both droplets were visually still hydrated on the bottom chip surface. For this experiment, the droplets were dispensed onto a 200-nm height spacer-chip, and the cell was sealed with a flat chip (windows aligned parallel) in order to set the liquid thickness to roughly the same as the MOF nanoparticles (200 nm). The spacer-chip was not subjected to plasma treatment to avoid the droplets spreading immediately after dispensing. However, the flat chip was plasma treated to help the spreading of the liquid upon sealing the cell and to create a mixing front within the window. Due to the surrounding water droplets, which create the high-humidity environment, sealing the cell is also likely to create some dilution in the NP solutions. However, for this experiment, demonstration of mixing was

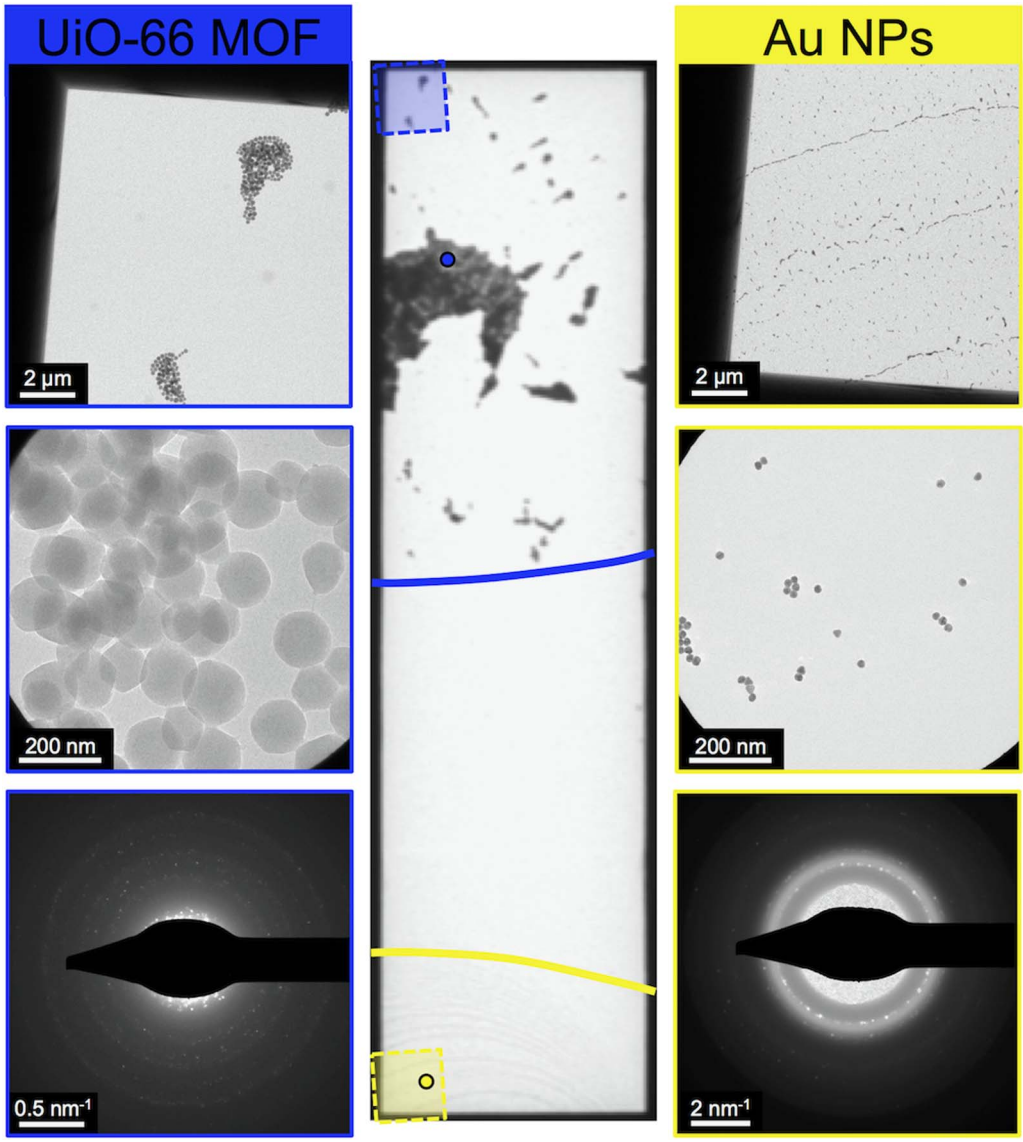

Figure 2. Transmission electron microscopy images of 200 nm UiO-66 (blue, left column) and 20 nm gold nanoparticles (AuNPs) (yellow, right column) dispensed onto a single window on a liquid cell and allowed to dry (chip from Figs. 1a–1c). The tall and narrow center image is a low-magnification image of the entire window area of the chip from Figure 1c after the deposited liquid droplets have completely dried at ambient conditions. The images in the left and right columns show clear separation between the UiO-66 and AuNPs, solvent edges for each solution are indicated by blue and yellow lines. The structures of each nanoparticle are also confirmed by selected area electron diffraction. Dashed line boxes indicate the regions where the top row images were recorded on the window. The small circles indicate the regions where the center row images and corresponding diffraction patterns were acquired. Note the difference in scale bars for selected area electron diffraction (SAED) patterns which is indicative of the large difference in Au and metal-organic-framework (MOF) lattice spacing.

the aim, rather than loading particles of a specific concentration. The liquid cell was then loaded into the microscope to start imaging within 7 min of sealing the cell. The imaging was performed intermittently at electron doses between $15.0\,e\,nm^2/s$ (6.7×10^5 Gy/s) and $0.2\,e\,nm^2/s$ (1.2×10^5 Gy/s) in order to limit beam damage. We have previously shown these dose rates are low enough to prevent beam damage to the MOFs (Patterson et al., 2015*a*), which are the more beam-sensitive materials in the experiment. We therefore believe that the beam has no effect on particle size or morphology, although some charging of the particles is likely to occur.

Initial imaging of the cell (Fig. 3) showed discrete areas of MOF nanocrystals at the "top" of the cell (Figs. 3a–3c), AuNPs at the "bottom" of the cell (Figs. 3e, 3f), and an area with initial mixing of the two components at the center of the cell (Fig. 3d). After ~30 min following cell assembly, we observed AuNPs (based on their distinctive size, morpho-

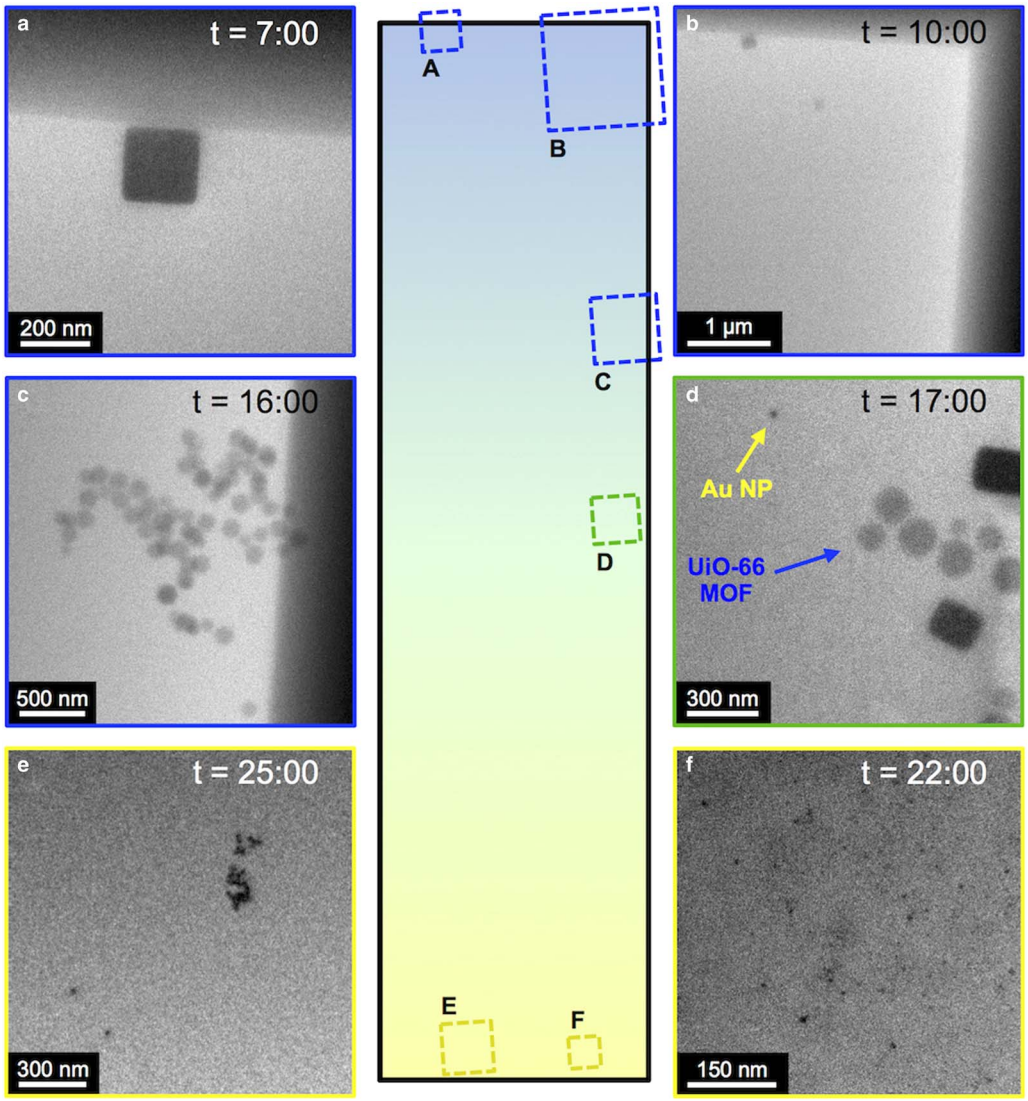

Figure 3. Transmission electron microscopy (TEM) images of a liquid cell sealed immediately after dispensing 200 nm UiO-66 (blue) and 20 nm gold nanoparticles (AuNPs) (yellow) onto opposite ends of the single window. The images show clear separation of the UiO-66 (**a–c**) with Au (**e,f**) as well as an initial mixing front (green) (**d**). *t* is the time after sealing the liquid cell. The tall narrow graphic in the center is a qualitative scheme of the liquid composition within the window region as observed over the first 20 min after sealing the cell. Yellow is pure AuNPs, blue is pure UiO-66 metal-organic-framework (MOF), and green is a mixed composition of Au and MOF. Labeled squares indicate the position on the window area where the respective TEM images (**a–f**) were acquired.

logy, and contrast) at the top of the cell mixed with the MOF nanoparticles (Fig. 4) indicating AuNP migration across the cell. The number of detected AuNPs at the top of the cell continued to increase over time during our observation. This observed movement/mixing is much slower than would be expected based on bulk diffusion of these nanomaterials, but is consistent with other recent work studying AuNP dynamics in a similar LCTEM assembly (Verch et al., 2015; Woehl & Prozorov, 2015). It is well known that near surface effects in the liquid cell can dramatically reduce diffusion rates (Zheng et al., 2009*a*; Proetto et al., 2014). Motion of individual AuNPs was observed, as well as their adherence to the surface of the MOFs, clear indicators of a fully hydrated cell (Supplementary Movie 2). No migration of MOF particles was observed to the bottom end (i.e., the location initially patterned with AuNPs) of the liquid cell. We recently reported that assembly of the liquid cell immediately after plasma treatment (as in these experiments) resulted in the observation of MOF particles stuck to the liquid cell windows, however, assembly of the cell 1–2 h post plasma treatment resulted in significant motion of particles inside the cell (Patterson et al., 2015*a*). Therefore, the lack of motion observed here was likely due to either their adherence to the plasma-treated SiN_x membrane and/or to their large size (roughly equal to the spacer height). Controlling particle motion inside the cell is of paramount importance

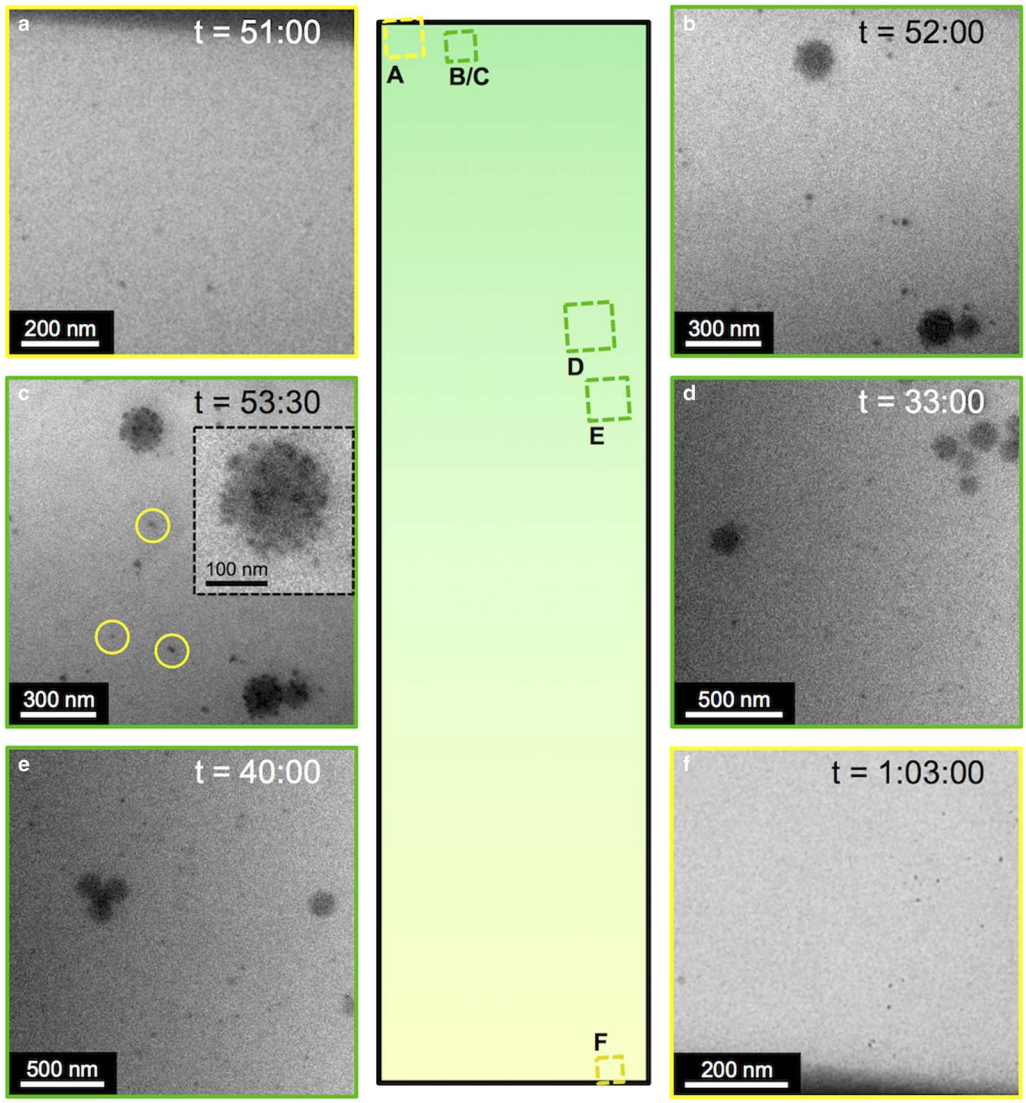

Figure 4. Transmission electron microscopy (TEM) images of the same liquid cell in Figure 3, after full diffusion and mixing of the UiO-66 (blue) and gold nanoparticles (AuNPs) (yellow) had occurred. The images show significant diffusion of Au into the UiO-66 end of the cell (**a–e**) and little or no diffusion of the metal-organic-frameworks (MOFs) into the Au end of the cell (**f**). *t* is the time after sealing the liquid cell. The tall narrow graphic in the center is a qualitative scheme of the liquid composition within the window region as observed 30 min after sealing the cell. Yellow is pure AuNPs, blue is pure UiO-66 MOF, and green is a mixed composition of Au and MOF (now the primary composition). Labeled squares indicate the position on the window area where the respective TEM images (**a–f**) were acquired. Image (**c**) was acquired at the same location as (**b**), 90 s later. Yellow circles in (**c**) indicate AuNPs that have diffused into the field of view and stuck to the top or bottom window during the 90-s time period from image (**b**).

for the observation of dynamics. Particles moving too quickly will not be able to be observed, either due to their motion exceeding the maximum framerate of the CCD camera, or due to decreased signal-to-noise when using high framerates. However, if particle motion is too slow, then the timescales over which mixing or dynamic process (e.g., particle collisions or interactions) will occur would exceed the threshold timescales related to beam damage. Further work in controlling particle *and indeed* small molecule motion in the cell is clearly needed (Patterson et al., 2015*b*). This should involve not only differences in plasma coating times, intensities, and surface aging, but also more permanent surface coatings and functionalization. Furthermore, detailed experiments involving controlled liquid thickness and beam doses are required. However, once this is achieved, controlled motion combined with the mixing procedures outlined here, would enable much more detailed experiments involving solution mixing and chemistry inside the cell. The ability to spot two different liquids at μm-scale separation distances on LCTEM chips greatly improves the probability for solution mixing over the viewing window for directly observing chemical reactions by LCTEM, and can

help overcome the limitations associated with sub-diffusion motion of nanomaterials inside liquid cells, shortening the imaging times (radiolysis doses) required to observe particle migration and mixing.

Supplementary Movie 2

Supplementary Movie 2 can be found online. Please visit journals.cambridge.org/jid_MAM.

Conclusion

These experiments demonstrate that automated picoliter drop-on-demand dispensing, combined with automated grid recognition and alignment in the SciTEM instrument, can be used to mix multiple solutions within the liquid cell, allowing assembly of liquid cells to observe nanoparticle migration and interaction, and potentially chemical reactions, while imaging in the microscope. Furthermore, using this dispensing technology and imaging strategy, one can conceive of many array designs where the mixing time of multiple different solutions could occur within one experiment. From a fundamental standpoint, technology for controlling the dispensing of low liquid volumes is essential for the advancement of LCTEM and this proof-of-concept shows the great potential to perform direct solution mixing and/or high-throughput *in situ* experiments. We intend this study as an initial demonstration of an approach that should enable researchers to study processes involving mixing of materials and/or reagents. In addition, the work should set the stage for the design and fabrication of novel chip designs to fully take advantage of picoliter dispensing techniques in combination with automated grid alignment in order to controllably load and mix solutions within the liquid cells.

Acknowledgments

The authors acknowledge support for this work from the AFOSR via a PECASE (FA9550-11-1-0105), ARO STIR W911NF-15-1-0080, and ARO W911NF-15-1-0189 to N.C.G. and via a AFOSR Basic Research Initiative grant (FA9550-12-1-0414), which enabled the purchase and operation of the UCSD LCTEM equipment. In addition, N.C.G. thanks the Alfred P. Sloan Foundation for a fellowship.

References

Aerni, H.-R., Cornett, D.S. & Caprioli, R.M. (2006). Automated acoustic matrix deposition for MALDI sample preparation. *Anal Chem* **78**(3), 827–834.

Barnhill, S.A., Bell, N.C., Patterson, J.P., Olds, D.P. & Gianneschi, N.C. (2015). Phase diagrams of polynorbornene amphiphilic block copolymers in solution. *Macromolecules* **48**(4), 1152–1161.

Calvert, P. (2001). Inkjet printing for materials and devices. *Chem Mater* **13**(10), 3299–3305.

Chen, Q., Cho, H., Manthiram, K., Yoshida, M., Ye, X. & Alivisatos, A.P. (2015*a*). Interaction potentials of anisotropic nanocrystals from the trajectory sampling of particle motion using in situ liquid phase transmission electron microscopy. *ACS Cent Sci* **1**(1), 33–39.

Chen, X., Li, C. & Cao, H. (2015*b*). Recent developments of the in situ wet cell technology for transmission electron microscopies. *Nanoscale* **7**(11), 4811–4819.

Choucair, A. & Eisenberg, A. (2003). Control of amphiphilic block copolymer morphologies using solution conditions. *Eur Phys J E Soft Matter* **10**(1), 37–44.

Cravillon, J., Schröder, C.A., Nayuk, R., Gummel, J., Huber, K. & Wiebcke, M. (2011). Fast nucleation and growth of ZIF-8 nanocrystals monitored by time-resolved in situ small-angle and wide-angle x-ray scattering. *Angew Chem Int Ed Engl* **50**(35), 8067–8071.

de Gans, B.-J., Duineveld, P.C. & Schubert, U.S. (2004). Inkjet printing of polymers: State of the art and future developments. *Adv Mater* **16**(3), 203–213.

de, J.N. & Ross, F.M. (2011). Electron microscopy of specimens in liquid. *Nat Nanotechnol* **6**(11), 695–704.

Evans, J.E., Jungjohann, K.L., Browning, N.D. & Arslan, I. (2011). Controlled growth of nanoparticles from solution with in situ liquid transmission electron microscopy. *Nano Lett* **11**(7), 2809–2813.

Li, J., Rossignol, F. & Macdonald, J. (2015). Inkjet printing for biosensor fabrication: Combining chemistry and technology for advanced manufacturing. *Lab Chip* **15**(12), 2538–2558.

Liao, H.-G. & Zheng, H. (2013). Liquid cell transmission electron microscopy study of platinum iron nanocrystal growth and shape evolution. *J Am Chem Soc* **135**(13), 5038–5043.

Liao, H.-G., Zherebetskyy, D., Xin, H., Czarnik, C., Ercius, P., Elmlund, H., Pan, M., Wang, L.-W. & Zheng, H. (2014). Facet development during platinum nanocube growth. *Science* **345**(6199), 916–919.

Mai, Y. & Eisenberg, A. (2012). Self-assembly of block copolymers. *Chem Soc Rev* **41**(18), 5969–5985.

Nielsen, M.H., Aloni, S. & De Yoreo, J.J. (2014). In situ TEM imaging of CaCO3 nucleation reveals coexistence of direct and indirect pathways. *Science* **345**(6201), 1158–1162.

Patterson, J.P., Abellan, P., Denny, M.S., Park, C., Browning, N.D., Cohen, S.M., Evans, J.E. & Gianneschi, N.C. (2015*a*). Observing the growth of metal–organic frameworks by in situ liquid cell transmission electron microscopy. *J Am Chem Soc* **137**(23), 7322–7328.

Patterson, J.P., Proetto, M.T. & Gianneschi, N.C. (2015*b*). Soft nanomaterials analysed by in situ liquid TEM: Towards high resolution characterisation of nanoparticles in motion. *Perspect Sci* **6**, 106–112.

Proetto, M.T., Rush, A.M., Chien, M.-P., Abellan Baeza, P., Patterson, J.P., Thompson, M.P., Olson, N.H., Moore, C.E., Rheingold, A.L., Andolina, C., Millstone, J., Howell, S.B., Browning, N.D., Evans, J.E. & Gianneschi, N.C. (2014*b*). Dynamics of soft nanomaterials captured by transmission electron microscopy in liquid water. *J Am Chem Soc* **136**(4), 1162–1165.

Smeets, P.J.M., Cho, K.R., Kempen, R.G.E., Sommerdijk, N.A.J.M. & De Yoreo, J.J. (2015). Calcium carbonate nucleation driven by ion binding in a biomimetic matrix revealed by in situ electron microscopy. *Nat Mater* (advance online publication).

Tekin, E., Smith, P.J. & Schubert, U.S. (2008). Ink-jet printing as deposition and patterning tool for polymers and inorganic particles. *Soft Matter* **4**(4), 703–713.

Verch, A., Pfaff, M. & de Jonge, N. (2015). Exceptionally slow movement of gold nanoparticles at a solid/liquid interface investigated by scanning transmission electron microscopy. *Langmuir* **31**(25), 6956–6964.

Williamson, M.J., Tromp, R.M., Vereecken, P.M., Hull, R. & Ross, F.M. (2003). Dynamic microscopy of nanoscale cluster growth at the solid-liquid interface. *Nat Mater* **2**(8), 532–536.

Wixforth, A., Strobl, C., Gauer, C., Toegl, A., Scriba, J. & v Guttenberg, Z. (2004). Acoustic manipulation of small droplets. *Anal Bioanal Chem* **379**(7–8), 982–991.

Woehl, T.J., Evans, J.E., Arslan, I., Ristenpart, W.D. & Browning, N.D. (2012). Direct in situ determination of the mechanisms controlling nanoparticle nucleation and growth. *ACS Nano* **6**(10), 8599–8610.

Woehl, T.J., Park, C., Evans, J.E., Arslan, I., Ristenpart, W.D. & Browning, N.D. (2014). Direct observation of aggregative nanoparticle growth: Kinetic modeling of the size distribution and growth rate. *Nano Lett* **14**(1), 373–378.

Woehl, T.J. & Prozorov, T. (2015). The mechanisms for nanoparticle surface diffusion and chain self-assembly determined from real-time nanoscale kinetics in liquid. *J Phys Chem C* **119**(36), 21261–21269.

Zheng, H., Claridge, S.A., Minor, A.M., Alivisatos, A.P. & Dahmen, U. (2009*a*). Nanocrystal diffusion in a liquid thin film observed by in situ transmission electron microscopy. *Nano Lett* **9**(6), 2460–2465.

Zheng, H., Smith, R.K., Jun, Y.-W., Kisielowski, C., Dahmen, U. & Alivisatos, A.P. (2009*b*). Observation of single colloidal platinum nanocrystal growth trajectories. *Science* **324**(5932), 1309–1312.